Functionalized Multi-Walled Carbon Nanotube based Sensors for Distributed Methane Leak Detection

Md Humayun*, R. Divan†, L. Stan†, D. Rosenmann†, D. Gosztola†, L. Gundel‡, P. A. Solomon§, I. Paprotny*
*Department of Electrical and Computer Engineering
University of Illinois at Chicago, Chicago, IL 60607
Email: paprotny@uic.edu
†Center for Nanoscale Materials, Argonne National Laboratory,Argonne IL 60439, USA
‡ Lawrence Berkeley National Laboratory, Berkeley, CA 94720
§U. S. Environmental Protection Agency, Las Vegas, NV 89199

***Abstract*—This paper presents a highly sensitive, energy efficient and low-cost distributed methane (CH_4) sensor system (DMSS) for continuous monitoring, detection and localization of CH_4 leaks in natural gas infrastructure such as transmission and distribution pipelines, wells, and production pads. The CH_4 sensing element, a key component of the DMSS, consists of a metal oxide functionalized multi-walled carbon nanotube (MWCNT) mesh which, in comparison to existing literature, shows stronger relative resistance change while interacting with lower ppm concentreation of CH_4. For the DMSS a Gaussian plume triangulation algorithm has been developed, which, given a geometric model of the surrounding environment, can precisely detect and localize a CH_4 leak as well as estimate its mass flow rate.**

I. Introduction

Despite having a shorter lifetime than CO_2, CH_4 is more efficient in trapping radiation [1], [2]. The impact of CH_4 on climate change is 25 times stronger than that of CO_2 over a 100-year period [1]. In 2013, 10% of emitted greenhouse gas in the USA was CH_4, while 29% of CH_4 emission was thermogenic, i.e., the source is man-made, such as natural gas and petroleum systems [2]. Hence, an extensive deployment of low cost, highly sensitive, selective and continuous CH_4 monitoring networks throughout the natural gas extraction and distribution infrastructure is of vital importance.

In this paper, we describe a low-cost microfabricated CH_4 sensing system and a corresponding detection algorithm for pinpointing the leaks in natural gas infrastructures. A leak detection algorithm for such low cost microfabricated networks of CH_4 sensors for natural gas distribution system has not been reported. Our novel Gaussian plume triangulation algorithm can precisely detect and localize a CH_4 leak and estimates its mass flow rate, if a geometric model of the surrounding environment is provided. This algorithm complements our novel metal oxide functionalized CNT mesh based microfabricated CH_4 sensing element which is the key constituent for the distributed CH_4 sensor system (DMSS).

II. Related Work

Three types of CH_4 sensors have been generally reported in literature: (a) sensors based on filtered infrared detection [3], (b) sensors based on Cavity Ring-Down Spectroscopy (CRDS) [4], (c) metal-oxide based chemo-resistor/chem-FET [5].

Filtered infrared sensors, which detect CH_4 in the ppm range from its absorption of infra-red light, have been widely used in gas gathering, transmission and distribution pipelines. The strongest optical absorption for CH_4 occurs around in the mid-IR region at a wavelength of 3.3 μm. A number of other hydrocarbon gases also have absorption bands/lines in the same spectral region, so a mid-IR system often responds to other hydrocarbons. Hence, mid-IR detectors are not methane-specific [3]. Also, mid-IR detectors are not inexpensive and often need to be cooled to achieve better signal-to-noise ratios, increasing their power consumption [3].

Sensors based on Cavity Ring-Down Spectroscopy (CRDS) utilize an optical detection scheme to conduct fast mobile leak measurements. The isotopic ratios of the stable isotopes of both carbon and hydrogen, along with the atmospheric concentration and distribution of the CH_4, can be used to derive the location and magnitude of CH_4 sources. However, the main use of this sensor is identifying the source(s) of large changes in CH_4 levels over a larger area than a leaked remote site; CRDS is not suitable for remote leak sensing [4].

CNT based gas sensors have the following properties which are uniquely attributed to their nano-scale dimension: (1) great adsorptive power due to large surface area to volume ratio, (2) stronger modulation of electrical properties (i.e., resistance) upon exposure to target gases, (3) tunable electrical properties correlated with composition and size, and (4) compatibility with low-power micro and nano-electronics [6], [7].

Thus parts per million (ppm) level of gas detection has been reported using CNT based chemoresistive sensors with a power consumption of only few mWs [8], [9].

978-1-4799-8203-5/15/$31.00 ©2015 IEEE

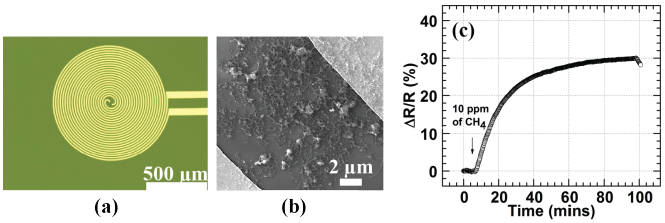

Fig. 1. (a) Optical microscope image of a functionalized MWCNT based CH_4 chemoresistor sensor, (b) Scanning electron microscope image of the sensor, and (c) Relative resistance change of the sensor as a function of time while the sensor was exposed to a mixture of 10 ppm of CH_4 in dry air inside an enclosed plastic chamber.

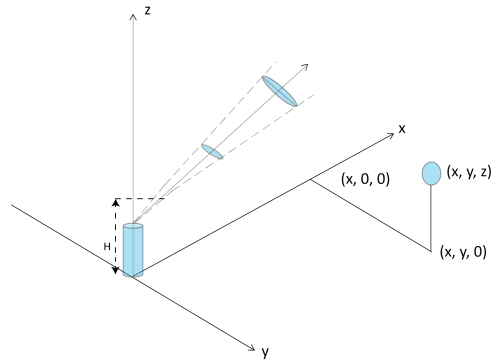

Fig. 2. Illustration of the Gaussian plume dispersion model.

III. Sensor Fabrication and Testing

We fabricated metal oxide functionalized multi-walled CNT (MWCNT) based CH_4 chemoresistor sensors which were able to detect 10 ppm of CH_4 in dry air at room temperature. A lift-off based photolithography process was implemented to fabricate a set of interdigitated metal (Au/Cr) electrodes on top of SiO_2/Si substrates (Fig. 1a). The gap between the electrodes varied in the range of 5 μm to 10 μm. A solution of MWCNTs/ethanol was drop deposited on the interdigitated electrodes following a baking at 75 °C temperature to remove the solvent. MWCNTs network was found to be trapped within the electrodes, making the electrodes electrically conducting (Fig. 1b). The MWCNTs were then surface-activated by O_2 plasma and UV-O_3 for duration of 5 mins to 1 hr. The surface pre-treated MWCNTs network was functionalized with various metal oxides using atomic layer deposition (ALD). The fabricated sensors were tested at room temperature inside an enclosed plastic chamber where 10 ppm CH_4 in dry air mixture was introduced while maintaining a constant relative humidity (RH) inside the test chamber. The relative resistance change of the sensor ($\Delta R/R = (R_{CH_4} - R_{air})/R_{air}$) were recorded as a function of time and was found to increase in a monotonic fashion (Fig. 1c).

IV. Triangulation Algorithm for the Distributed Sensors

In this work, we present a novel Gaussian plume triangulation algorithm which, given a geometric model of the surrounding environment, can precisely detect and localize a CH_4 leak while estimating the mass flow rate.

In the below example the DMSS nodes are assumed distributed on a 5 m $\times$ 5 m grid, however, the DMSS can be extended to an arbitrary sensor distribution. The approach relies on a varying wind direction to sweep a plume of CH_4 emanating from a nearby leak across two or more sensors. Using the National Wind Technology Center dataset [10] as a baseline, we analyzed wind rose plots for 4 randomly chosen 18 days period in 2013. We found the average (prevailing) direction of wind is West or South-West and the wind covers more than 180° in the course of 18 days. This variation in wind directions is later used by the leak detection algorithm.

We have devised a Gaussian plume model (GPM) for estimating the evolution of the plume emanating from a ground level leak for different wind directions and speeds. For a constant leak rate and a constant wind speed the ground level concentration χ (μg/m^3) at the point (x,y) may be written using the Gaussian plume equation as [11]:

$$\chi(x, y, z_0, H) = \frac{Q \times 10^6}{\pi \sigma_y \sigma_z U} exp[-\frac{1}{2}(\frac{y}{\sigma_y})^2] \times exp[-\frac{1}{2}(\frac{H}{\sigma_z})^2] \quad (1)$$

where Q is the source emission rate (g/s), U is the wind speed at stack height, σ_y and σ_z are the standard deviation of concentration distributions in crosswind and vertical directions respectively, H is the effective stack height (the sum of stack height and plume rise), x is the downwind distance from the stack, y is the crosswind distance from the plume centerline, and z_0 is the vertical distance from ground level, assumed to be zero.

From the fitting of Pasquill-Gifford-Turner (PGT) diffusion coefficient curves , σ_y and σ_z were found to be:

$$\sigma_y = cx^d \quad (2)$$

$$\sigma_z = ax^b \quad (3)$$

where, constants a, b, c, and d are 0.112, 0.91, 0.197, and 0.908, respectively. Fig. 2 shows an illustration of the Gaussian plume dispersion model terminology. Note that although the GPM might not be applicable (due to turbulence) during high ($>$ 6 m/s) wind velocities, such wind speeds are uncommon, and sensor readings during those times will be ignored without significantly compromising the 18 day detection time. Similarly, the readings at wind speeds below 1 m/s will be omitted.

If valid, the Gaussian plume distribution at a point x downstream of the leak is uniquely defined by the dispersion parameters, which are assumed constant, the wind velocity U and the emission rate at the leak Q.

Once a plume moves across a sensor location due to variations in wind direction, a plume distribution can be reconstructed. This concept is illustrated on Fig. 3. As CH_4

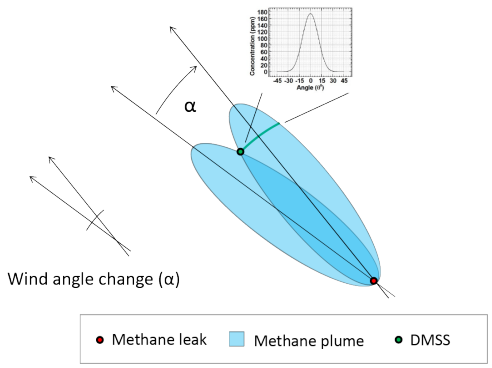

Fig. 3. Illustration of the CH_4 plume propagating across a DMSS node due to varying wind direction. This example assumes that wind velocity is constant as the angle varies.

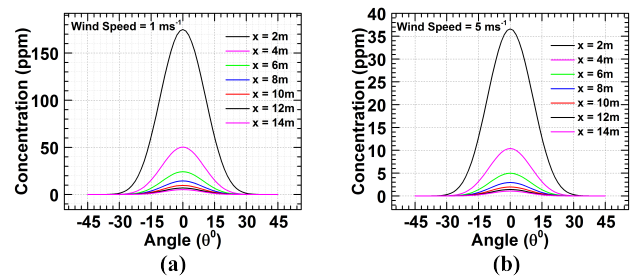

Fig. 4. Distribution of CH_4 plume as a function of rotation of the wind direction for two different wind velocities: (a) 1 ms^{-1} and (b) 5 ms^{-1}. Each plot shows different distance along the centerline of the plume (2m − 14m). The leak rate was assumed to be 1.9 g/min which corresponds to 6 standard cubic feet per hour (SCFH).

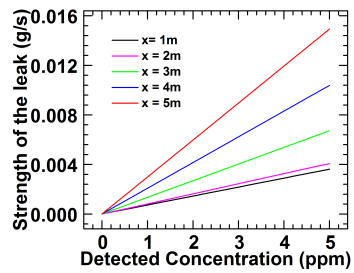

Fig. 5. Strength of the leak (g/s) as a function of maximum detected CH_4 concentration by a DMSS located at different distances along the centerline of the plume.

plume from a nearby leak rotates from position i) to position ii), the sensor signal records the plume profile. The below analysis assumes the wind velocity is constant, which may not be the case; however the theory extends easily to cases with variable wind velocity.

Calculated distributions of a CH_4 plume using Eq. (1) are plotted on Fig. 4 as a function of rotating wind direction for two different wind velocities (1 ms^{-1} and 5 $^{-1}$). The down-wind coordinate (x) from the leak (the distance to the sensor from the leak along the centerline of the plume), can be extrapolated from the peak concentration λ and wind velocity U by numerically solving the following equation:

$$log(ca) + (b+d)logx = log\frac{QV_m \times 10^3}{M\lambda\pi U} - \frac{(\Delta h)^2}{2a^2x^{2b}} \quad (4)$$

where, λ is the concentration of the detected CH_4 in ppm, M is the Molar mass of CH_4 (g/mol, V_m is the molar volume of an ideal gas at standard temperature and pressure. The plume rise due to the buoyancy of CH_4 (Δh) is calculated as

$$\Delta h = \frac{Ex^{\beta}}{\overline{u^{\alpha}}} \quad (5)$$

where, for a stable atmosphere, $\alpha = 1$, $\beta = 2/3$, and $E = 1.6F^{(1/3)}$, where F is the buoyancy flux parameter, defined as

$$F = \frac{gd^2V_s(T_s - T_a)}{4T_s} \quad (6)$$

where g is acceleration due to gravity (9.8 ms^{-2}), d is stack diameter, V_s is stack exit velocity, T_a is ambient temperature at stack height, and T_s is stack exit temperature at stack height.

Once distance to the leak (x) is established, the following formula can be used to calculate the leakage rate:

$$Q = \frac{\lambda M}{V_m} \times \frac{\pi\sigma_y\sigma_z U}{10^6} \times exp[\frac{1}{2}(y/\sigma_y)^2] \times exp[\frac{1}{2}(H/\sigma_z)]^2 \quad (7)$$

where Q is the mass flow rate (MFR) of the leak. Consequently, estimation of the MFR of a single leak is possible by scanning the leak distribution plume.

The mass flow rate (MFR) of the leak (g/s) as a function of maximum detected CH_4 concentration by a DMSS located at different distances along the centerline of the plume is illustrated in Fig. 5.

The shape of the actual plume recorded by the DMSS nodes depends on its lower detection limit (LDL), or sensitivity. We are currently achieving single ppm CH_4 sensitvity using our functionalized MWCNT based chemoresistor sensor. The projected sensitivity of the DMSS sensor element is 0.1 ppm with one minute integration time, with anticipated LDL of 0.5 to 1 ppm. Assuming a quantization error of 1 ppm, an error in plume height, as well as plume width will be manifested. Other factors, such as wind speed/wind direction error (e.g. direction assumed to be $\pm 3°$.) will also contribute to error estimation at the sensor node, but can be eliminated in part by increasing integration time. Fig. 6 shows the center point plume concentration as a function of wind speed (1 − 5 ms^{-1}) and distance for a point leak at 6 standard cubic feet per hour (SCFH). The error bars showing the quantization at 8 m distance from the leak are shown. (Note 7 m is the largest distance from the leak at a 5 m × 5 m grid.)

Similarly, the LDL quantization and sensor noise will result in a cross-wind uncertainty, which will expand the area where

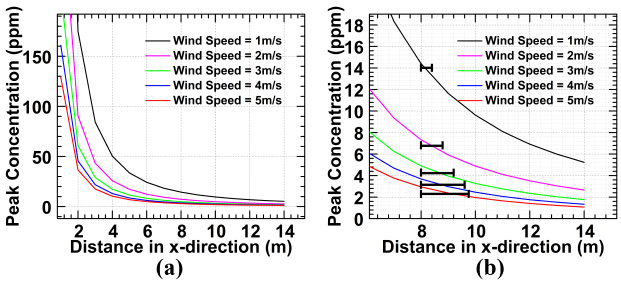

Fig. 6. (a) Peak concentration of the plumes at different distances along the centerline (2 m − 14 m) at various wind speeds ($1\text{ms}^{-1} - 5\text{ ms}^{-1}$) (b) Peak concentration of the plumes at different distances along the centerline (7 m 14 m) at various wind speeds ($1\text{ ms}^{-1} - 5\text{ ms}^{-1}$). The error bars correspond to uncertainty in distance to sensor due to LDL quantization, assuming an effective LDL of 1 ppm.

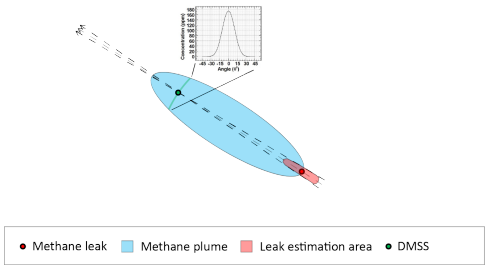

Fig. 7. Estimation of the leak location based on the shape of the plume as it sweeps across the DMSS node. LDL and sensor error quantifies the error, which then results in a leak estimation area (LEA) confining the position of the leak.

the leak can potentially be located. This uncertainty overlaps with the uncertainty in the wind direction, which usually is around $\pm 2°$. We assume a combined error of $\pm 3°$ to account for the variability of the sensing of the CH_4 plume in the cross wind direction. The resulting leak location is estimated as confined to an area, rather than an exact location. This area is called the leak estimation area (LEA) and the CH_4 leak can be confined to be located anywhere within the area. Fig. 7 shows this concept, where a plume that scanned over a DMSS sensor is used to estimate LEA. Based on the quantization error, uncertainty, the leak can be provably confined to with the leak estimation area.

LEA can be bounded by a rectangle, with its major axis aligned with the down-wind direction, while the minor axis aligned with the cross-wind direction. Furthermore, signal from multiple sensors will help to reduce the sensor noise, and improve the accuracy of the signal. Estimating LEA from multiple sensors is shown on Fig. 8.

V. Conclusion

We have fabricated a functionalized MWCNT based CH_4 chemoresistor sensor capable of sensing below 10 ppm of CH_4 in dry air at room temperature. We presented a Gaussian plume model (GPM) based algorithm for a distributed methane sensor system (DMSS) which can use our chemoresistor sensor to localize leaks in natural gas infrastructure, such as production wells and pads. We present a localization algorithm, which

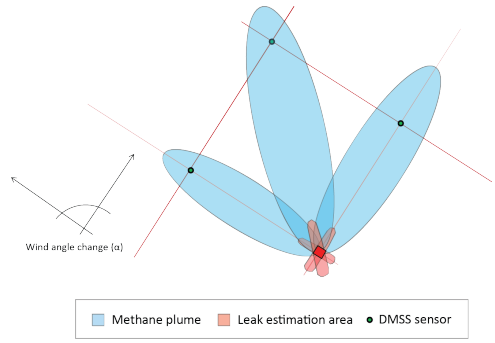

Fig. 8. Overlapping LEAs (annotated in bright red) of a CH_4 plume sweeping multiple sensor locations. Note that the wind might change, and thus vary the size of the plume. The overlapping LEA is greatly reduced, and for the proposed ATMOS node distribution can be shown to be less than 1 m × 1 m.

can be used with the distributed sensors to pinpoint CH_4 leaks, allowing the DMSS to be used for continuous low-cost monitoring of CH_4 emission. Together with energy harvesting and ultra-low power wireless solutions the DMSS can be used for ubiquitous monitoring of natural gas infrastructure.

Acknowledgment

Use of the Center for Nanoscale Materials, Argonne National Laboratory, an Office of Science user facility, was supported by the U. S. Department of Energy, Office of Science, Office of Basic Energy Sciences, under Contract No. DE-AC02-06CH11357. The project is in part funded by the College of Engineering, University of Illinois, Chicago, IL.

References

[1] Climate change 2007: Working group i: The physical science basis. [Online]. Available: http://www.ipcc.ch/publications_and_data/ar4/wg1/en/ch2s2-10-2.html

[2] Overview of greenhouse gases. [Online]. Available: http://epa.gov/climatechange/ghgemissions/gases/ch4.html

[3] C. Massie, G. Stewart, G. McGregor, and J. R. Gilchrist, "Design of a portable optical sensor for methane gas detection," *Sens. and Act. B: Chem.*, vol. 113, no. 2, pp. 830–836, 2006.

[4] Measurement of the carbon isotopic ratio of atmospheric methane. [Online]. Available: http://cfpub.epa.gov/ncer_abstracts/index.cfm/fuseaction/display.abstractDetail/abstract/6351/report/0

[5] P. Fau, M. Sauvan, S. Trautweiler, C. Nayral, L. Erades, A. Maisonnat, and B. Chaudret, "Nanosized tin oxide sensitive layer on a silicon platform for domestic gas applications," *Sens. and Act. B: Chem.*, vol. 78, no. 1, pp. 83–88, 2001.

[6] T. Zhang, S. Mubeen, N. V. Myung, and M. A. Deshusses, "Recent progress in carbon nanotube-based gas sensors," *Nanotech.*, vol. 19, no. 33, p. 332001, 2008.

[7] M. Dresselhaus, G. Dresselhaus, and R. Saito, "Physics of carbon nanotubes," *Carbon*, vol. 33, no. 7, pp. 883–891, 1995.

[8] Y. Lu, J. Li, J. Han, H.-T. Ng, C. Binder, C. Partridge, and M. Meyyappan, "Room temperature methane detection using palladium loaded single-walled carbon nanotube sensors," *Chem. Phys. Lett.*, vol. 391, no. 4, pp. 344–348, 2004.

[9] G. Lu, L. E. Ocola, and J. Chen, "Room-temperature gas sensing based on electron transfer between discrete tin oxide nanocrystals and multiwalled carbon nanotubes," *Advanced Materials*, vol. 21, no. 24, pp. 2487–2491, 2009.

[10] National wind technology center. [Online]. Available: http://www.nrel.gov/midc/nwtc_m2/

[11] S. N. P. J. H. Seinfeld, *Atmospheric Chemistry and Physics: From Air Pollution to Climate Change*, 2nd ed. John Willey and Sons, 2006.